




## ORIGINAL ARTICLE

# A New Strategy for Adult T-Cell Leukemia Treatment Targeting Glycogen Synthase Kinase-3 $\beta$

Chie Ishikawa<sup>1,2</sup> | Naoki Mori<sup>1</sup> 

<sup>1</sup>Department of Microbiology and Oncology, Graduate School of Medicine, University of the Ryukyus, Nishihara, Japan | <sup>2</sup>Division of Health Sciences, Transdisciplinary Research Organization for Subtropics and Island Studies, University of the Ryukyus, Nishihara, Japan

**Correspondence:** Naoki Mori (naokimori50@gmail.com)

**Received:** 18 April 2024 | **Revised:** 16 August 2024 | **Accepted:** 18 August 2024

**Keywords:** 9-ING-41 | adult T-cell leukemia | glycogen synthase kinase-3 $\beta$  | human T-cell leukemia virus type 1

## ABSTRACT

**Objectives:** The role of glycogen synthase kinase (GSK)-3 $\beta$  in adult T-cell leukemia (ATL) caused by human T-cell leukemia virus type 1 (HTLV-1) is paradoxical and enigmatic. Here, we investigated the role of GSK-3 $\beta$  and its potential as a therapeutic target for ATL.

**Methods:** Cell proliferation/survival, cell cycle, apoptosis, and reactive oxygen species (ROS) generation were examined using the WST-8 assay, flow cytometry, and Hoechst 33342 staining, respectively. Expression of GSK-3 $\beta$  and cell cycle/death-related proteins, and survival signals was analyzed using RT-PCR, immunofluorescence staining, and immunoblotting.

**Results:** HTLV-1-infected T-cell lines showed nuclear accumulation of GSK-3 $\beta$ . GSK-3 $\beta$  knockdown and its inhibition with 9-ING-41 and LY2090314 suppressed cell proliferation/survival. 9-ING-41 induced G2/M arrest by enhancing the expression of  $\gamma$ H2AX, p53, p21, and p27, and suppressing the expression of CDK1, cyclin A/B, and c-Myc. It induced caspase-mediated apoptosis by decreasing the expression of Bcl-xL, Mcl-1, XIAP, c-IAP1/2, and survivin, and increasing the expression of Bak and Bax. 9-ING-41 also induced ferroptosis and necroptosis, promoted JNK phosphorylation, and suppressed IKK $\gamma$  and JunB expression. It inhibited the phosphorylation of I $\kappa$ B $\alpha$ , Akt, and STAT3/5, induced ROS production, and reduced glycolysis-derived lactate levels.

**Conclusion:** GSK-3 $\beta$  functions as an oncogene in ATL and could be a potential therapeutic target.

## 1 | Introduction

Adult T-cell leukemia (ATL) is a mature T-cell malignancy caused by the retrovirus, human T-cell leukemia virus type 1 (HTLV-1) [1–4], which is endemic to the Southwest Japan, South America, the Caribbean islands, Intertropical Africa, Central Australia, the Middle East, and Romania [2–4]. ATL is characterized by hepatosplenomegaly, lymphadenopathy, skin lesions, hypercalcemia, presence of leukemic cells with multilobulated nuclei in blood, and organ involvement, including that of the central nervous system and gastrointestinal tract [2–4]. It is classified into indolent (smoldering and favorable chronic) and aggressive (acute, lymphoma, and unfavorable chronic) types [2–4]. Patients with aggressive ATL have a median survival

time of less than 1 year, mainly because of resistance to conventional chemotherapy and significant immunosuppression [2–4]. Although mechanisms underlying HTLV-1 transformation have been extensively studied, ATL remains an unmet medical need.

ATL occurs in approximately 5% of HTLV-1-infected adult individuals [4]. HTLV-1 encodes the oncogenic protein, Tax. It affects intercellular signaling pathways including the NF- $\kappa$ B pathway and regulates the transcription of several genes involved in the oncogenic processes, playing a crucial role in ATL initiation [1, 3]. However, Tax is not detected in most ATL cases [3].

Glycogen synthase kinase (GSK)-3, a serine/threonine kinase with two isoforms  $\alpha$  and  $\beta$ , was discovered as a key enzyme

in glycogen metabolism [5]. The two isoforms are highly homologous, but have different tissue-specific functions and substrates [5–8]. GSK-3 phosphorylates more than 100 protein substrates that are components of many key cellular pathways and, therefore, has a widespread impact on normal cells and diseases. GSK-3 $\beta$  is recognized for its paradoxical roles in cancer. It functions as a tumor promoter or suppressor depending on the cell type and phosphorylation status. The enzymatic activity of GSK-3 $\beta$  is mediated by differential phosphorylation of its serine 9 (inactive form) and tyrosine 216 (active form) residues. Serine 9 is phosphorylated by Akt, PKA, p70S6K, and p90RSK, whereas tyrosine 216 is autophosphorylated or phosphorylated by Src tyrosine kinase. GSK-3 $\beta$  primes oncogene products for proteasomal degradation, mainly through proliferative pathways such as Wnt/ $\beta$ -catenin, and can, thereby, serve as a tumor suppressor. In contrast, GSK-3 $\beta$  overexpression has been reported in several tumors, where it functions as a tumor promoter. GSK-3 $\beta$  is actively involved in multiple signaling pathways including the NF- $\kappa$ B pathway, which is related to the proliferation and survival of cancer cells. To date, several GSK-3 $\beta$  inhibitors have been developed and used in cancer clinical trials.

GSK-3 $\beta$  is involved in signaling pathways in ATL, as it regulates the Wnt/ $\beta$ -catenin pathway [9]. Hsp90 inhibitors, which are effective in preclinical ATL models [9–11], suppress Akt activity, thereby, activating GSK-3 $\beta$ , which then phosphorylates, ubiquitinates, and degrades  $\beta$ -catenin [9]. This indicates the anti-ATL effect of Hsp90 inhibitors on ATL via GSK-3 $\beta$  activation. GSK-3 $\beta$  is, therefore, a potential tumor suppressor in ATL. However, we have been investigating whether GSK-3 $\beta$  is an oncogene. Recently, a case of refractory ATL with a significant and sustained response to monotherapy with 9-ING-41, a GSK-3 $\beta$  inhibitor in the clinical phase, was published [12]. Here, we investigated the potential mechanisms underlying the anti-ATL activity of GSK-3 $\beta$  inhibition.

## 2 | Materials and Methods

### 2.1 | Cell Culture

The HTLV-1-transformed T-cell lines, MT-2, MT-4, SLB-1, and HUT-102; the ATL-derived T-cell lines, MT-1 and TL-OmI; and the HTLV-1-negative T-cell line, Jurkat, were grown in RPMI-1640 medium (Nacalai Tesque, Inc., Kyoto, Japan) supplemented with 10% heat-inactivated fetal bovine serum (Biological Industries, Kibbutz Beit Haemek, Israel) and 1% penicillin/streptomycin (Nacalai Tesque, Inc.). Human peripheral blood mononuclear cells (PBMCs) obtained from healthy donors were purchased from Precision for Medicine (Frederick, MD, USA).

### 2.2 | Compounds

9-ING-41 was purchased from ChemScene (Monmouth Junction, NJ, USA). LY2090314, ferrostatin-1 (a ferroptosis inhibitor), and deferoxamine mesylate were purchased from Cayman Chemical (Ann Arbor, MI, USA). Necrostatin-1

(a necroptosis inhibitor) and z-VAD-FMK (a pan-caspase inhibitor) were purchased from Abcam (Cambridge, UK) and Promega Corp. (Madison, WI, USA), respectively. Phytohemagglutinin (PHA) was purchased from Sigma-Aldrich Co., LLC (St. Louis, MO, USA).

### 2.3 | siRNA-Based Gene Knockdown of GSK-3 $\beta$

MT-2 cells were transfected with either a predesigned double-stranded GSK-3 $\beta$  siRNA (ON-TARGET plus SMART pool; Dharmacon, Inc., Lafayette, CO, USA) or siCONTROL non-targeting siRNA pool (Dharmacon, Inc.) by pulsing twice at 1100V for 30ms using a Microporator MP-100 device (Digital Bio Technology, Seoul, Korea).

### 2.4 | Water-Soluble Tetrazolium (WST)-8 Assay

The WST-8 (Nacalai Tesque, Inc.) assay was performed according to the manufacturer's instructions to determine cell toxicity and growth inhibition. Briefly, cells were seeded in 96-well plates. At the end of each set of experiments, 10 $\mu$ L of the WST-8 reagent was added to each well, and the cells were incubated for 4h. To detect metabolically intact cells, the absorbance at 450nm was measured using a Wallac 1420 Multilabel Counter (PerkinElmer, Inc., Waltham, MA, USA). The drug concentration required to inhibit the WST-8 activity by 50% (IC<sub>50</sub>) was assessed using the CalcuSyn software (version 2.0; Biosoft, Cambridge, UK).

### 2.5 | Cell Cycle Analysis

To assess cell cycle progression, cells were treated with either 0.25 $\mu$ M 9-ING-41 or DMSO (solvent control; Nacalai Tesque, Inc.) for 24h and stained with propidium iodide using the CycleTEST Plus DNA Reagent kit (Becton-Dickinson Immunocytometry Systems, San Jose, CA, USA). The cell cycle was analyzed using an SH800 Cell Sorter (Sony Biotechnology, Inc., Tokyo, Japan) by measuring the propidium iodide fluorescence of individual nuclei. The percentage of cells in each cell cycle phase was determined using the Kaluza Analysis software (version 2.1; Beckman Coulter, Inc., Marseille, France).

### 2.6 | Apoptosis Assays

Cells were treated with either DMSO or increasing concentrations of 9-ING-41 for 48h. They were then collected and permeabilized by incubation with digitonin and subsequently stained with phycoerythrin-conjugated APO2.7 antibody (Beckman Coulter, Inc.) to measure the expression of mitochondrial membrane protein 7A6, resulting from apoptosis [13]. The percentage of APO2.7-positive cells was measured using flow cytometry on an SH800 Cell Sorter (Sony Biotechnology, Inc.). Changes in nuclear morphology were assessed by observing cells stained with Hoechst 33342 (Dojindo Molecular Technologies, Inc., Kumamoto, Japan)

under a DMI6000 microscope (Leica Microsystems, Wetzlar, Germany).

## 2.7 | Caspase Assay

The APOPCYTO Caspase Colorimetric Assay kits (Medical & Biological Laboratories Co.) were used to measure caspase-3, -8, and -9 activation, according to the manufacturer's instructions. Briefly, the cells were treated with DMSO or 0.5  $\mu$ M 9-ING-41 for 48 h. Thereafter, the cells were lysed with cell lysis buffer provided in the kit. The release of the chromophore  $\rho$ -nitroanilide from the substrates after cleavage was quantified using a Wallac 1420 Multilabel Counter (Perkin Elmer). The relative caspase activity was calculated as the ratio of the colorimetric output for the treated and control samples, the latter being set to 1.

## 2.8 | Reverse Transcriptase (RT)-PCR

For gene expression analysis, total RNA was extracted from cultured cells using TRIzol reagent (Invitrogen Life Technologies, Carlsbad, CA, USA). The total RNA (1  $\mu$ g) was reverse transcribed into first-strand cDNA using a PrimeScript RT-PCR kit (Takara Bio, Inc., Otsu, Japan). This cDNA was used as a template for amplifying the target gene *GSK-3 $\beta$*  and reference gene *GAPDH* using the corresponding primers, which were as follows: 5'-GCCCGACTAACACCACTG-3' (sense) and 5'-CCACGGTCTCCAGTATTA-3' (antisense) for *GSK-3 $\beta$*  and 5'-GCCAAGGTCATCCATGACAACCTTTGG-3' (sense) and 5'-GCCTGCTCACCACCTTCTTGATGTC-3' (antisense) for *GAPDH*. The thermocycling parameters were as follows: initial denaturation at 94°C for 2 min, followed by 30 cycles at 94°C for 30 s for denaturation, 56°C for 30 s for annealing, and 72°C for 30 s for extension, and a final cumulative amplification at 72°C for 10 min.

## 2.9 | Western Blot Analysis

9-ING-41-treated cells were collected and lysed in lysis buffer, as described previously [14]. The protein levels were quantified using the DC Protein Assay kit (Bio-Rad Laboratories, Inc., Hercules, CA, USA). Equal amounts of proteins were electrophoresed on 8%, 10%, 12%, and 15% sodium dodecyl sulfate-polyacrylamide gels, and the separated proteins were transferred onto polyvinylidene difluoride membranes (Merck KGaA, Darmstadt, Germany). The membranes were then incubated with specific primary antibodies. Subsequently, the membranes were incubated with horseradish peroxidase-conjugated secondary antibodies and proteins were visualized using an enhanced chemiluminescence reagent (Amersham Biosciences Corp., Piscataway, NJ, USA). Actin served as an internal control. Primary antibodies against glycogen synthase (GS), phospho-GS (Ser641), Bcl-xL, Bax, Bak, survivin, cellular inhibitor of apoptosis (c-IAP) 1, H2AX, phospho-H2AX (Ser139), cyclin-dependent kinase (CDK) 1, phospho-I $\kappa$ B $\alpha$  (Ser32/36), IKK $\gamma$ , phospho-Akt (Ser473), phospho-JNK (Thr183/Tyr185), phospho-STAT3 (Tyr705), phospho-STAT5 (Tyr694), cleaved poly(ADP-ribose)

polymerase (PARP), cleaved caspase-8 and -3, as well as horseradish peroxidase-conjugated secondary anti-mouse and anti-rabbit IgG antibodies, were purchased from Cell Signaling Technology, Inc. (Beverly, MA, USA). Antibodies against cyclin A, cyclin B, and actin were purchased from Neomarkers, Inc. (Fremont, CA, USA). Antibodies against X-linked inhibitor of apoptosis protein (XIAP) and c-Myc were purchased from Medical & Biological Laboratories Co., Ltd. (Nagoya, Japan) and Wako Pure Chemical Industries (Osaka, Japan), respectively. Antibodies against GSK-3 $\beta$ , phospho-GSK-3 $\beta$  (Ser9), phospho-GSK-3 $\beta$  (Tyr216), GSK-3 $\alpha$ , c-IAP2, myeloid cell leukemia-1 (Mcl-1), p21, p27, p53, JunB, and JunD were purchased from Santa Cruz Biotechnology, Inc. (Dallas, TX, USA). Lt-4, an antibody against Tax [15] was provided by Dr Yuetsu Tanaka (University of the Ryukyus, Okinawa, Japan). Lt-4 recognizes epitopes located between amino acids 94–179 and those that are dependent on the secondary or tertiary structures of the Tax antigen [16].

## 2.10 | Immunofluorescence Staining

Indirect immunofluorescence staining was performed as described previously [17]. The cells were fixed with 4% paraformaldehyde and permeabilized with Triton X-100 on microscope slides. The slides were then incubated overnight with mouse primary antibody against GSK-3 $\beta$  (Santa Cruz Biotechnology, Inc.) at 4°C and subsequently with goat anti-mouse secondary antibody (labeled with Alexa Fluor 488, Invitrogen Life Technologies, Carlsbad, CA, USA) at 25°C for 2 h. After washing, nuclei were counterstained with Hoechst33342. Immunostaining was visualized using a confocal laser-scanning microscope (DMI6000).

## 2.11 | Intracellular ROS Detection

Intracellular ROS levels were measured using flow cytometry with the fluorescent probe CellROX Green reagent (Thermo Fisher Scientific, Waltham, MA, USA). Briefly, the treated cells were collected and incubated with 750 nM of this reagent for 60 min. The labeled cells were washed once with phosphate-buffered saline (PBS) and suspended in PBS. CellROX-induced fluorescence was analyzed using an SH800 Cell Sorter (Sony Biotechnology, Inc.).

## 2.12 | Measurement of Lactate Production

Cell culture supernatants were collected. Lactate levels were measured using the lactate assay kit-WST (Dojindo Molecular Technologies), employing a Wallac 1420 Multilabel Counter (Perkin Elmer), according to the manufacturer's instructions.

## 2.13 | Statistical Analysis

Results are presented as the mean  $\pm$  standard deviation (SD). In all figures, SD is indicated by an error bar. Statistical analysis was performed using Student's *t*-test or analysis of variance with the Tukey–Kramer test.  $p < 0.05$  was considered to indicate statistically significant results.

### 3 | Results

#### 3.1 | Aberrant Expression of GSK-3 $\beta$ in HTLV-1-Infected T-Cell Lines

To determine whether GSK-3 could be an effective therapeutic target for ATL, the expression of GSK-3 $\alpha$  and  $\beta$  in normal PBMCs, HTLV-1-transformed T-cell lines, ATL-derived T-cell lines, and an uninfected T-cell line was investigated. HTLV-1-infected T-cell lines had higher levels of GSK-3 $\beta$  compared with normal PBMCs and uninfected Jurkat cells (Figure 1A). Using the Lt-4 antibody, we identified p40, a 40-kDa molecule, and p68 (a fusion protein between the envelope and the Tax-coding sequence). Unlike ATL-derived T-cell lines, HTLV-1-transformed T-cell lines expressed Tax (Figure 1A). These results indicate that the expression of GSK-3 $\beta$  is enhanced in HTLV-1-infected T-cell lines, irrespective of Tax expression. In contrast, GSK-3 $\alpha$  levels were not enhanced in HTLV-1-infected T-cell lines. Notably, PHA stimulation induced both GSK-3 $\alpha$  and  $\beta$ . Next, we

localized GSK-3 $\beta$  in HTLV-1-transformed MT-2 and MT-4 cells and ATL-derived MT-1 cells using immunofluorescence analysis and found it to accumulate in the nucleus (Figure 1B).

#### 3.2 | Impaired Proliferation of HTLV-1-Infected T Cells Upon GSK-3 $\beta$ Knockdown

Given that GSK-3 $\beta$  is overexpressed in HTLV-1-infected T-cell lines and is involved in multiple signaling pathways important for cellular functions, we investigated whether GSK-3 $\beta$  functionally supports the proliferation of these cells. To this end, we transiently knocked down GSK-3 $\beta$  using siRNA. siRNA-GSK-3 $\beta$  reduced GSK-3 $\beta$  expression in HTLV-1-infected MT-2 cells compared with that in control siRNA-treated cells (Figure 1C). Furthermore, the WST-8 assay results showed that GSK-3 $\beta$  knockdown significantly inhibited cell proliferation by 14% after 24 h and by 17% after 48 h of transfection in MT-2 cells compared with the proliferation of control siRNA-transfected cells (Figure 1D).

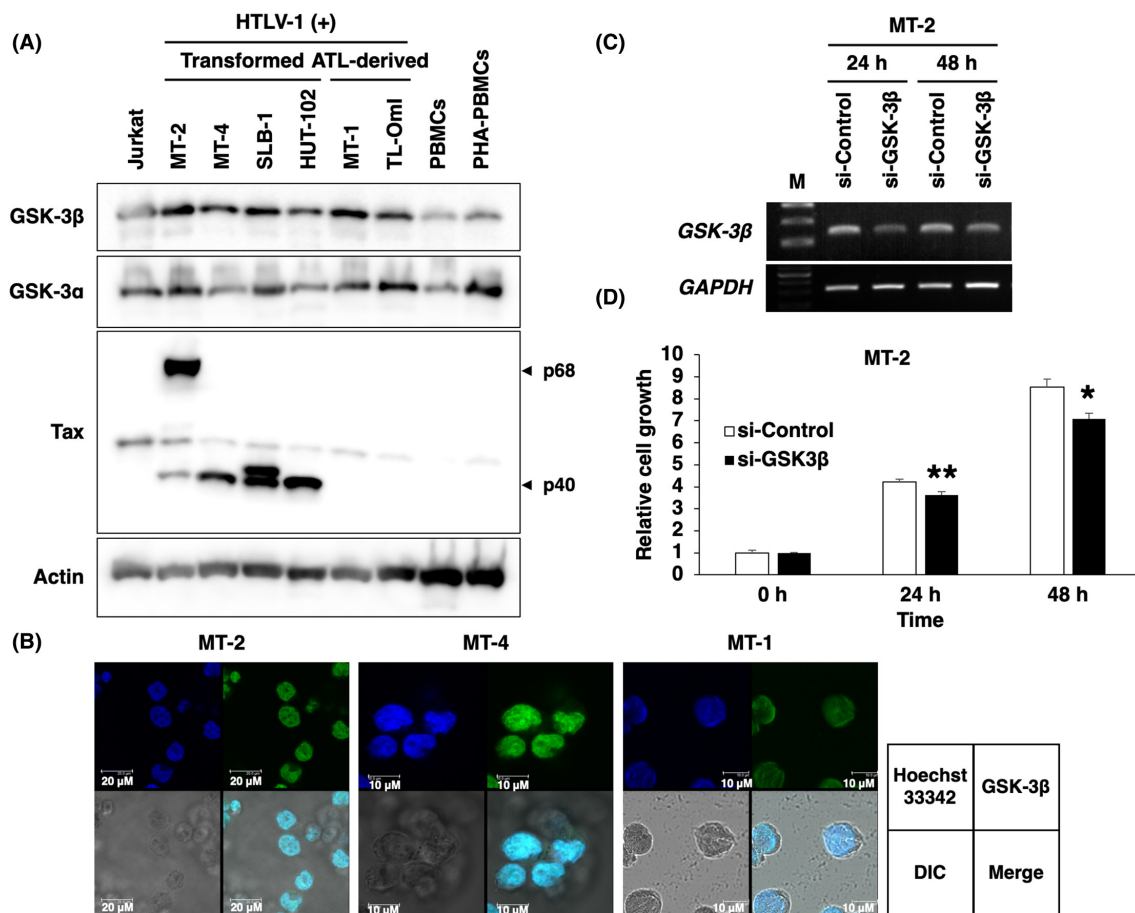


**FIGURE 1** | Glycogen synthase kinase (GSK)-3 $\beta$  is overexpressed in HTLV-1-infected T cells compared with that in uninfected T cells, and its downregulation causes growth retardation. (A) Expression of GSK-3 and Tax in uninfected Jurkat cells, HTLV-1-transformed T-cell lines, ATL-derived T-cell lines, normal peripheral blood mononuclear cells (PBMCs), and phytohemagglutinin (PHA)-stimulated PBMCs (PHA-PBMCs). Cells were harvested and processed for western blot analysis. (B) Immunofluorescence analysis of GSK-3 $\beta$  in HTLV-1-infected T cells. Blue: Hoechst 33342; green: GSK-3 $\beta$  labeled with Alexa Fluor 488-conjugated secondary antibody. Scale bars, 10 or 20  $\mu$ m. (C) RT-PCR analysis of GSK-3 $\beta$  mRNA expression in HTLV-1-infected MT-2 cells, showing the response to siRNA-GSK-3 $\beta$ . The cells were transfected with GSK-3 $\beta$  or control siRNA and collected after 24 and 48 h of transfection. GSK-3 $\beta$  mRNA levels in cells after GSK-3 $\beta$  knockdown were determined using RT-PCR. GAPDH was used as a control. (D) GSK-3 $\beta$  siRNA inhibited the proliferation of MT-2 cells. Growth of cells transfected with GSK-3 $\beta$  or control siRNA was assessed after 24 and 48 h of transfection using the WST-8 assay. The results are presented as the mean  $\pm$  SD of triplicates. \* $p$  < 0.005 and \*\* $p$  < 0.001, compared with values for cells transfected with control siRNA.

### 3.3 | GSK-3 $\beta$ Inhibition Reduces Proliferation and Survival of HTLV-1-Infected T-Cell Lines

HTLV-1-transformed and ATL-derived T-cell lines were treated with 9-ING-41 [12]. Treatment with 9-ING-41 for 24–72 h reduced the proliferation and viability of all HTLV-1-infected T-cell lines in a concentration- and time-dependent manner (Figure 2A). The IC<sub>50</sub> after 72 h was 77–636 nM. In contrast, the proliferation and viability of uninfected Jurkat cells and PBMCs from a healthy volunteer were unaffected even at 2  $\mu$ M 9-ING-41. These data indicate that 9-ING-41 specifically inhibits the proliferation and survival of HTLV-1-infected T cells without affecting uninfected T cells or normal PBMCs. To confirm whether GSK-3 $\beta$  inhibition by the small molecule was indeed successful, the levels of phospho-GSK-3 $\beta$  Tyr216 (activated form) in MT-2 cells were measured using western blot analysis (Figure 2B). Phospho-GSK-3 $\beta$  Tyr216 was suppressed by this inhibitor, whereas inhibitory phosphorylation of GSK-3 $\beta$  Ser9 was increased. Furthermore, the phosphorylation at Ser641 of GS, a direct downstream substrate of GSK-3 $\beta$ , was inhibited by 9-ING-41, indicating normal inhibitory effects of GSK-3 $\beta$  on GS. These results suggest that the anti-ATL activity of this 9-ING-41 is directly related to its inhibitory effect on GSK-3 $\beta$  activity. We surmised that if the inhibition of GSK-3 $\beta$  alone was adequate for the anti-ATL activity of 9-ING-41, a structurally unrelated selective inhibitor of GSK-3 $\beta$  would exhibit comparable anti-ATL effects. We, therefore, examined the impact of the GSK-3 $\beta$  inhibitor, LY2090314 [18]. LY2090314 led to a decrease in the proliferation and viability of HTLV-1-infected T-cell lines, including ATL-derived MT-1 cells (Figure 2C).

### 3.4 | GSK-3 $\beta$ Inhibition Blocks G2/M Progression of HTLV-1-Infected T Cells

The finding that 9-ING-41 inhibits cell proliferation led us to investigate its effect on cell cycle kinetics using flow cytometry. After 24 h of treatment with 9-ING-41, the cell population in the G2/M phase increased in MT-2 cells, coinciding with a reduction in the proportion of cells in the G1 phase, when compared with that in the control group, suggesting cell cycle arrest at G2/M (Figure 2D). To determine whether cell cycle arrest was affected by DNA damage, the expression of the DNA damage marker, histone H2AX phosphorylated at Ser139 ( $\gamma$ H2AX), was examined.  $\gamma$ H2AX expression was increased when cells were treated with 9-ING-41 (Figure 2E). Furthermore, the levels of proteins associated with cell cycle arrest, including p53, p21, and p27, were increased in a concentration-dependent manner after 9-ING-41 treatment compared with those in control cells. Conversely, the expression of CDK1, cyclin A, cyclin B, and c-Myc decreased in a concentration-dependent manner after 9-ING-41 treatment (Figure 2E).

### 3.5 | 9-ING-41 Induces Apoptosis, Ferroptosis, and Necroptosis

We determined whether 9-ING-41 could induce apoptosis besides inhibiting the growth of HTLV-1-infected T-cell lines. Fluorescence microscopy of 9-ING-41-treated cells stained with Hoechst 33342, a fluorescent DNA-staining dye, revealed typical characteristics

of apoptosis including nuclear condensation and fragmentation (Figure 3A). APO2.7 staining followed by flow cytometric analysis revealed that the proportion of apoptotic cells increased upon 9-ING-41 treatment in a dose-dependent manner (Figure 3B). This was confirmed using western blotting, wherein 9-ING-41 induced the cleavage of PARP, a hallmark of apoptosis (Figure 3C). Cleaved caspase-3 levels, which indicate the level of PARP cleavage, as well as cleaved caspase-8 levels, increased with increasing 9-ING-41 concentrations (Figure 3C). Treatment with 9-ING-41 increased the activities of caspase-3, -8, and -9, indicating the occurrence of apoptosis (Figure 3D). Moreover, we investigated whether activation of caspases was associated with 9-ING-41-induced cell death. Pretreatment with the pan-caspase inhibitor z-VAD-FMK significantly inhibited 9-ING-41-induced cell death (Figure 4A).

As the cytotoxic effect of 9-ING-41 was partially reversed by pretreatment with z-VAD-FMK, we further investigated caspase-independent nonapoptotic cell death caused by 9-ING-41. To further confirm whether 9-ING-41-induced cell death was involved in ferroptosis and necroptosis, we used necrostatin-1 and ferrostatin-1. Both inhibitors significantly inhibited 9-ING-41-mediated reduction in cell viability in HTLV-1-infected T cells (Figure 4B). As ferroptosis is an iron-dependent nonapoptotic cell death [19], we determined the effect of iron on the 9-ING-41-induced cell death. Pretreatment with lysosomal iron chelator deferoxamine significantly rescued the 9-ING-41-induced decrease in cell viability (Figure 4B), indicating the iron-dependency of 9-ING-41-induced cell death. These results indicate that in addition to caspase-dependent apoptosis, nonapoptotic pathways may also be involved in 9-ING-41-induced HTLV-1-infected T-cell death.

### 3.6 | 9-ING-41 Affects the Expression of Apoptosis-Regulatory Proteins

We determined the levels of apoptosis-related proteins using immunoblotting. Treatment of MT-2 and MT-4 cells with 9-ING-41 led to a dose-dependent decrease in expression of the antiapoptotic IAP and Bcl-2 family proteins, XIAP, c-IAP1, c-IAP2, Mcl-1, and Bcl-xL (Figure 5). Survivin expression was also downregulated in MT-4 cells. In contrast, 9-ING-41 upregulated the levels of the proapoptotic proteins, Bak and Bax. These results indicate that GSK-3 $\beta$  is central in mediating cell survival, mainly by promoting the expression of antiapoptotic proteins and suppressing the expression of proapoptotic proteins.

### 3.7 | Inhibition of GSK-3 $\beta$ Induces ROS Generation, JNK Activation, and Suppression of Glycolysis and the NF- $\kappa$ B, Akt, AP-1, and STAT3/5 Pathways

ROS generation mediates DNA damage and plays an important role in many types of cancer cell death [20]. Therefore, the effect of 9-ING-41 on ROS generation in HTLV-1-infected T cells was investigated (Figure 6A). 9-ING-41 increased ROS generation indicating that ROS signaling is associated with 9-ING-41-induced cell death.

As GSK-3 $\beta$  is a key enzyme in glucose metabolism, we reasoned that this inhibitory effect occurred via regulation of glycolysis, an important metabolic pathway in cancer cells [21]. A

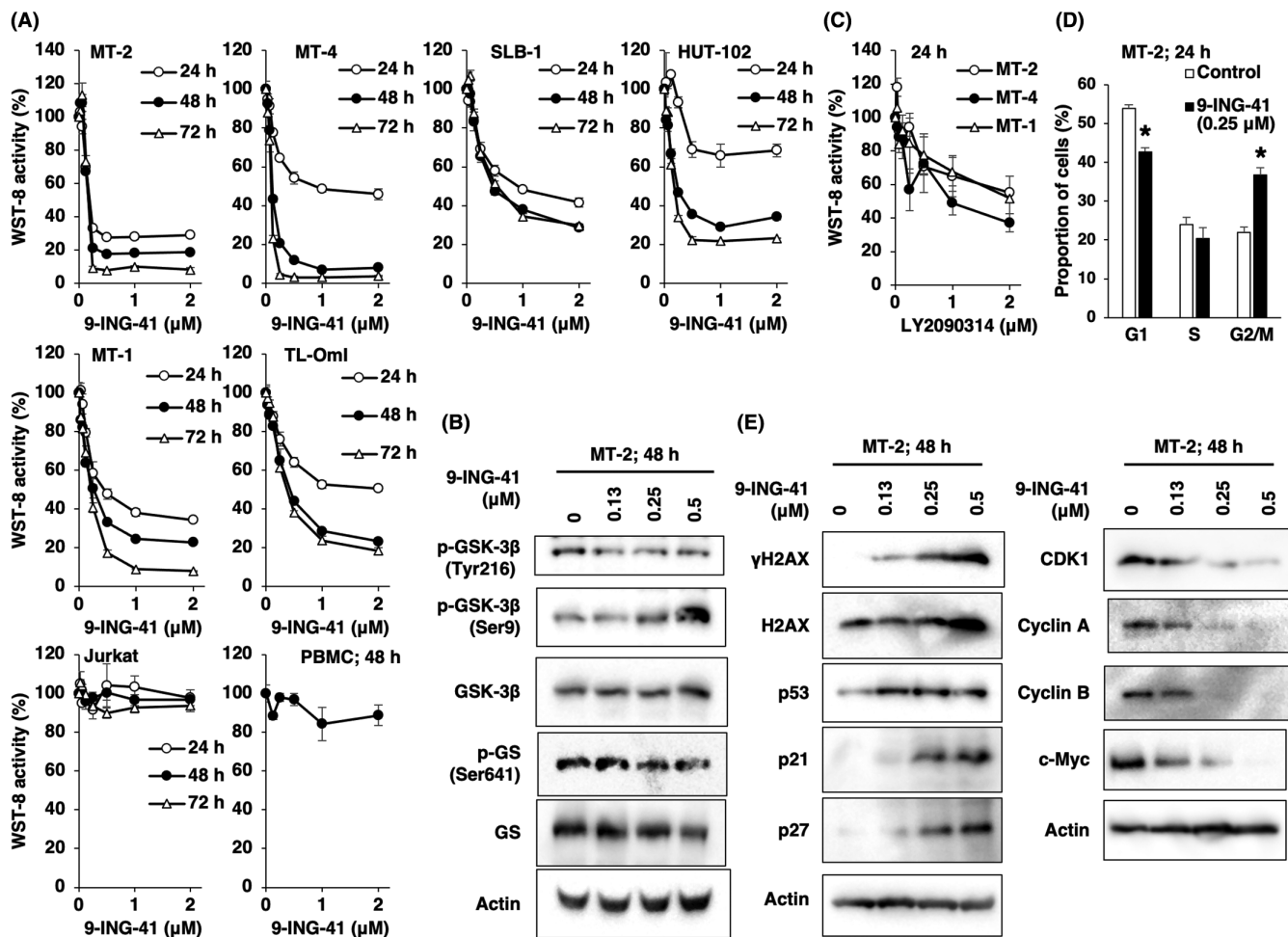


**FIGURE 2** | Glycogen synthase kinase (GSK)-3 $\beta$  inhibition results in reduction of the proliferation and survival of HTLV-1-infected T-cell lines. (A) The indicated cell lines were treated with different concentrations of the GSK-3 $\beta$  inhibitor 9-ING-41 for 24–72 h. Proliferation and survival were assessed using the WST-8 assay at different time points as indicated. (B) Changes in the phosphorylation of GSK-3 $\beta$  at Tyr216 and Ser9 and of GS at Ser641 caused by 9-ING-41. MT-2 cells were treated with the indicated concentrations of 9-ING-41 for 48 h and protein levels were quantitated using western blot analysis. (C) LY2090314, another GSK-3 $\beta$  inhibitor, led to a decrease in the proliferation and viability of HTLV-1-infected T-cell lines. The indicated cell lines were treated with different concentrations of LY2090314 for 24 h. Proliferation and survival were assessed using the WST-8 assay. (D) Bar graph shows results of the cell cycle analysis of MT-2 cells exposed to 9-ING-41 for 24 h. The data in (A), (C), and (D) represent the mean  $\pm$  SD of triplicates. \* $p < 0.0005$ , compared with the control. (E) Treatment with 9-ING-41 affected the expression of cell cycle-regulatory proteins in MT-2 cells. Actin was used as a loading control.

dose-dependent reduction in the levels of lactate, the product derived from glucose in the glycolysis, was observed in both MT-2 and MT-4 cells upon 9-ING-41 treatment (Figure 6B). Thus, inhibition of GSK-3 $\beta$  had an inhibitory effect on metabolic processes in HTLV-1-infected T cells.

Finally, we investigated whether 9-ING-41 could modulate signaling pathways in HTLV-1-infected T cells (Figure 6C). Treatment of MT-2 cells with different concentrations of 9-ING-41 for 48 h resulted in suppression of phosphorylation of I $\kappa$ B $\alpha$ , Akt, and STAT3/5. In contrast, this treatment induced JNK phosphorylation. Furthermore, the expression of IKK $\gamma$  and an AP-1 transcription factor component JunB, was suppressed by 9-ING-41 treatment. Thus, inhibition of GSK-3 $\beta$  contributes to the death of HTLV-1-infected T cells via suppression of IKK–NF- $\kappa$ B, Akt, AP-1, and STAT3/5 activity essential for the survival of HTLV-1-infected T cells and activation of JNK. The ATL-derived T-cell line MT-1, which does not express Tax, exhibits

constitutively active NF- $\kappa$ B but not Akt and STAT3/5 [22]. 9-ING-41 suppressed I $\kappa$ B $\alpha$  phosphorylation and IKK $\gamma$  expression in MT-1, as observed for MT-2 cells (Figure 6D).

#### 4 | Discussion

GSK-3 $\alpha$  and  $\beta$  are functionally related multifunctional serine/threonine protein kinases involved in several signaling pathways that support the growth of hematological malignancies [23]. Various GSK-3 $\beta$  inhibitors that compete with ATP have been designed and synthesized, but only three small molecule inhibitors, 9-ING-41, LY2090314, and CHIR98014, are currently in clinical trials for cancer [5, 24, 25]. 9-ING-41 is selective for GSK-3 among more than 320 other related kinases by at least one order of magnitude [5]. Recently, GSK-3 $\beta$  was identified as a potential therapeutic target for ATL in clinical trials [12]. However, the mechanisms underlying the clinical activity of

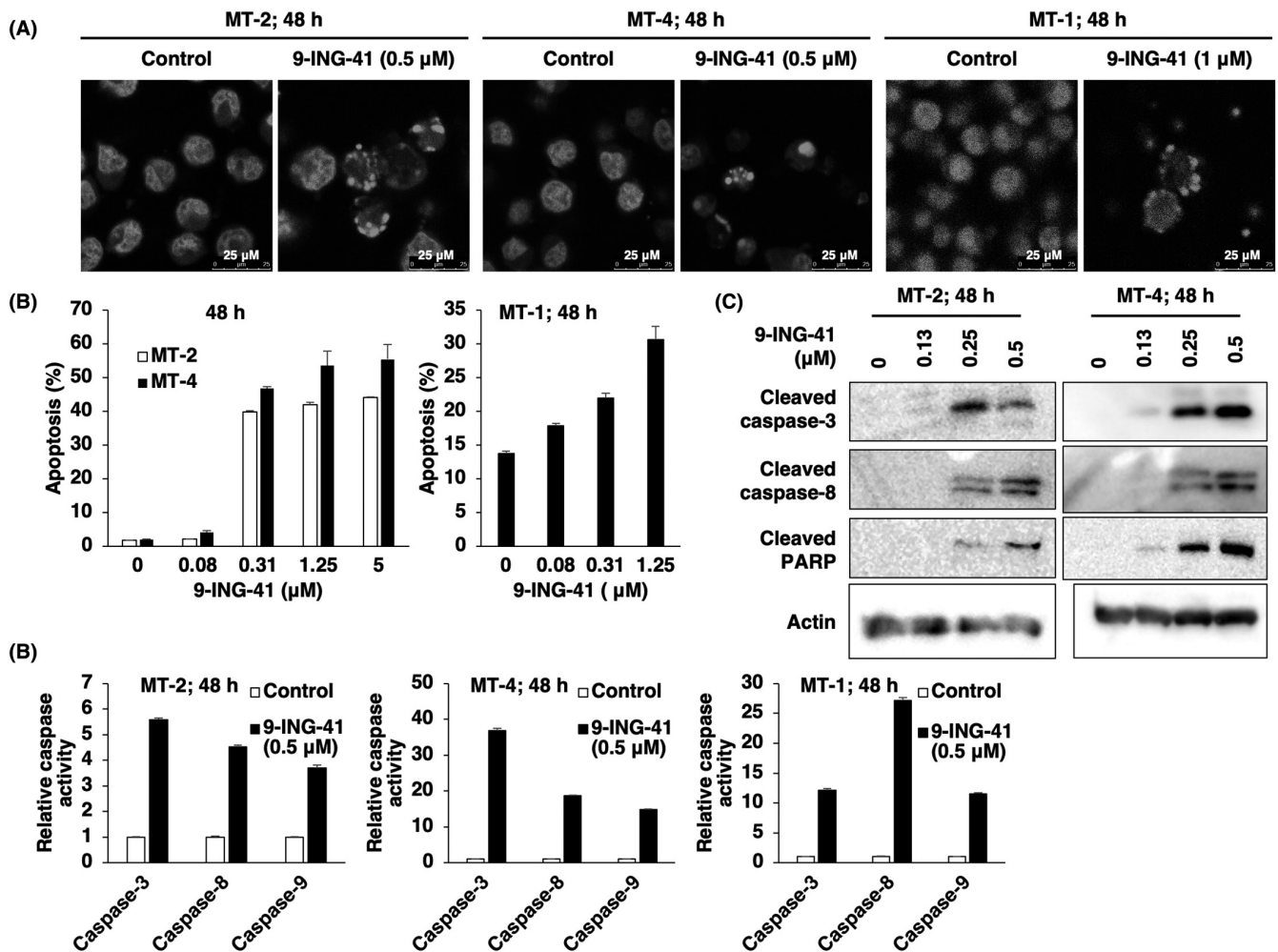


**FIGURE 3** | 9-ING-41 induces caspase-mediated apoptosis in HTLV-1-infected T-cell lines. (A) MT-2, MT-4, and MT-1 cells were treated with the indicated concentrations of 9-ING-41 for 48 h. Apoptosis induction following 9-ING-41 treatment was confirmed using nuclear staining with Hoechst 33342. Scale bar: 25  $\mu$ m. (B) APO2.7 staining was detected using flow cytometry. Apoptosis rates in the HTLV-1-infected T-cell lines were analyzed after 48 h of treatment with increasing concentrations of 9-ING-41. (C) Levels of cleaved caspases and PARP in MT-2 and MT-4 cells treated with 9-ING-41 for 48 h were determined using western blotting. Actin was used as a loading control. (D) Caspase-3, -8, and -9 activities were detected using APOPCYTO Caspase Colorimetric Assay kits. The data in (B) and (D) represent the mean  $\pm$  SD of triplicates.

9-ING-41 remain unclear. Here, we show that GSK-3 $\beta$ , but not  $\alpha$ , is overexpressed in HTLV-1-infected T-cell lines compared with that in uninfected Jurkat T-cell line and normal resting PBMCs. Inhibition of GSK-3 $\beta$  activity by 9-ING-41 and LY2090314, or siRNA-mediated knockdown inhibited the proliferation and survival of HTLV-1-infected T-cell lines. 9-ING-41 treatment induced cell cycle arrest and cell death. These results indicated that GSK-3 $\beta$  is important for the proliferation and survival of HTLV-1-infected T cells.

We observed cell cycle inhibition in the G2/M phase in HTLV-1-infected T cells treated with 9-ING-41. The expression of the cell cycle regulatory proteins cyclin A, cyclin B, and CDK1 was downregulated by GSK-3 $\beta$  inhibition. In the G2/M transition, CDK1 binds to cyclin A and enables mitosis initiation, whereas CDK1-cyclin B activation initiates and completes mitosis [26]. Our results suggest that GSK-3 $\beta$  positively regulates the expression of cyclin A, cyclin B, and CDK1 and that treatment with 9-ING-41 results in cell cycle arrest at the G2/M phase in HTLV-1-infected T cells. p53 elicits G2 checkpoint

responses through transcriptional upregulation of its downstream target gene *p21* [27]. p21 and p27 can inhibit the activities of the CDK1-cyclin A and CDK1-cyclin B complexes [28]. GSK-3 $\beta$  induces degradation of p53 and p21 [8]. c-Myc induces the expression of CDK1, cyclin A, and cyclin B, and represses the expression of p21 and p27 [28]. c-Myc expression is transcriptionally repressed by p53 [29]. Our results indicate that 9-ING-41 induced c-Myc downregulation, as previously reported [30]. Therefore, we suggest that cell cycle arrest in the G2/M phase by 9-ING-41 is associated with increased expression of p53 and decreased expression of c-Myc. p53 can also mediate apoptosis through the upregulation of Bak and Bax, downregulation of survivin, and inhibition of the activities of antiapoptotic Bcl-2 family proteins [31]. 9-ING-41 induced JNK activation and ROS production. JNK is an important mediator of ROS-induced apoptosis and the ROS-JNK pathway activates p53 [20].

The importance of the prosurvival activity of the NF- $\kappa$ B, Akt, AP-1, and STAT3/5 pathways in HTLV-1-infected T cells has

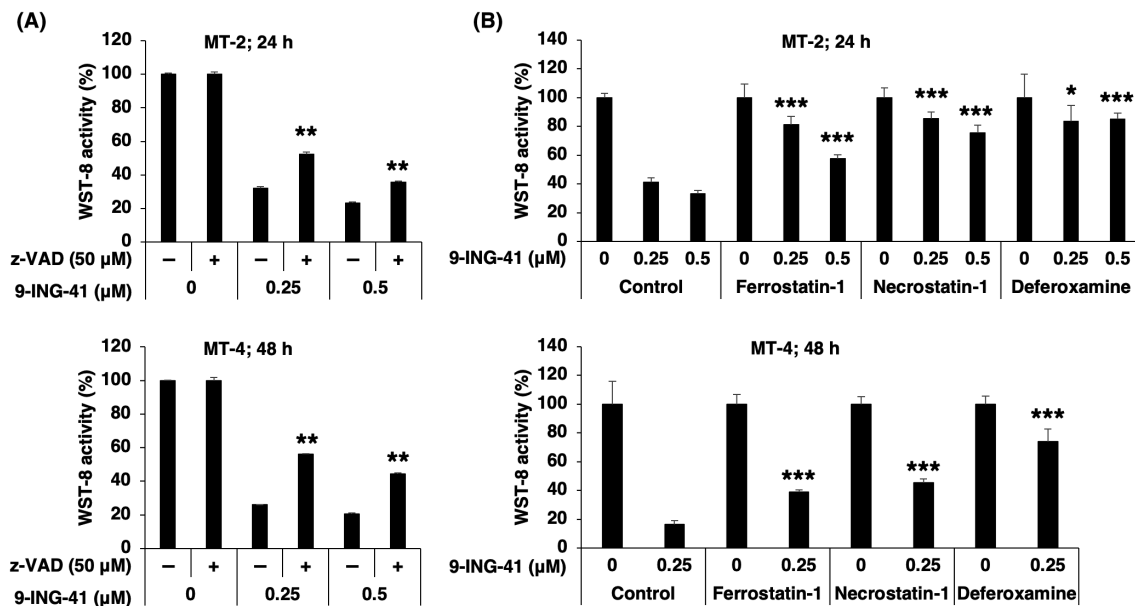


**FIGURE 4** | 9-ING-41-induced caspase-dependent and -independent cell death. (A) Pretreatment with z-VAD-FMK, a pan-caspase inhibitor, significantly inhibited 9-ING-41-induced cell death. MT-2 and MT-4 cells were pretreated with 50 μM z-VAD-FMK for 1 h and then treated with the indicated concentrations of 9-ING-41 for 24 or 48 h. (B) Ferroptosis and necroptosis are involved in 9-ING-41-induced cell death. Cells were pretreated with 50 μM ferrostatin-1, necrostatin-1, or deferoxamine for 1 h, followed by treatment with the indicated concentrations of 9-ING-41 for 24 or 48 h. Cell viability was assessed using the WST-8 assay. Data represent the mean ± SD of triplicates. \* $p < 0.005$ , \*\* $p < 0.001$ , and \*\*\* $p < 0.0005$ , compared with the control.

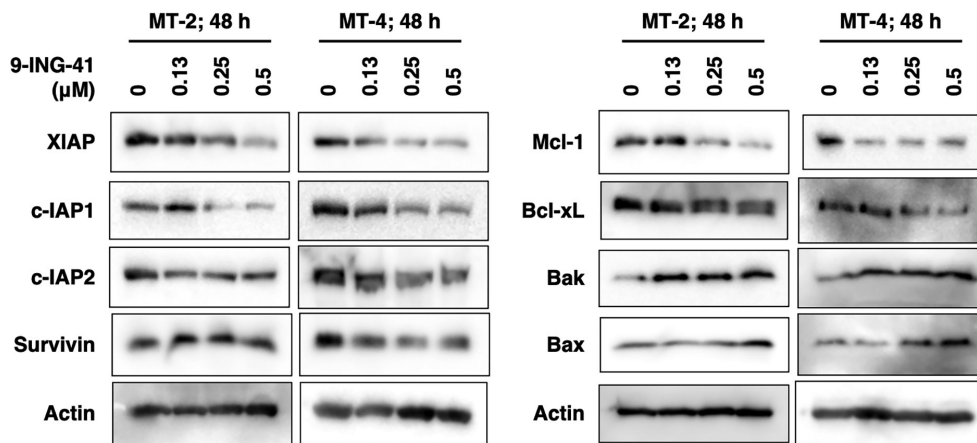


**FIGURE 5** | The effect of 9-ING-41 on the expression of apoptosis-related proteins. MT-2 and MT-4 cells were treated with the indicated concentrations of 9-ING-41 for 48 h. After treatment, whole-cell lysates were prepared and the proteins were immunoblotted. Actin was used as a loading control.

been reported [32–34]. The AP-1 transcription factors, JunB and JunD, in HTLV-1-infected T cells comprise AP-1 [14]. We observed that 9-ING-41 suppressed the expression of antiapoptotic proteins, including XIAP, c-IAP1/2, survivin, Mcl-1, and Bcl-xL, which are targets of these pathways [32, 35–37]. We also found that 9-ING-41 inhibited the expression of IKKγ and JunB, and the phosphorylation of IκBα, Akt, and STAT3/5, which suggests that GSK-3β regulates the NF-κB, Akt, AP-1, and STAT3/5 pathways. GSK-3β phosphorylates and stabilizes IKKγ and, thereby, the phosphorylation and degradation of IκBα and enhancement of NF-κB levels [38]. GSK-3β also phosphorylates and inactivates PTEN, resulting in increased Akt activation [39]. Furthermore, GSK-3β phosphorylates and activates STAT3/5 [40–42]. In contrast, NF-κB contributes to JunB expression [43]. Treatment

with 9-ING-41 suppressed the expression of JunB, but not of JunD, which indicates that NF-κB is involved in JunB expression in HTLV-1-infected T cells. Whether the effect of 9-ING-41 on NF-κB, Akt, AP-1, and STAT3/5 activity is mediated by direct phosphorylation of IKKγ, PTEN, and STAT3/5 and/or through crosstalk between NF-κB and AP-1 remains to be investigated. 9-ING-41 suppressed IκBα phosphorylation and IKKγ expression in MT-1 cells, as observed for MT-2 cells, suggesting that GSK-3β may contribute to the activation of the NF-κB pathway in Tax-negative ATL cells.

Targeting nonapoptotic forms of cell death, including necroptosis and ferroptosis, can have therapeutic effects on apoptosis-resistant cancer cells [44]. Indeed, GSK-3β inhibition can



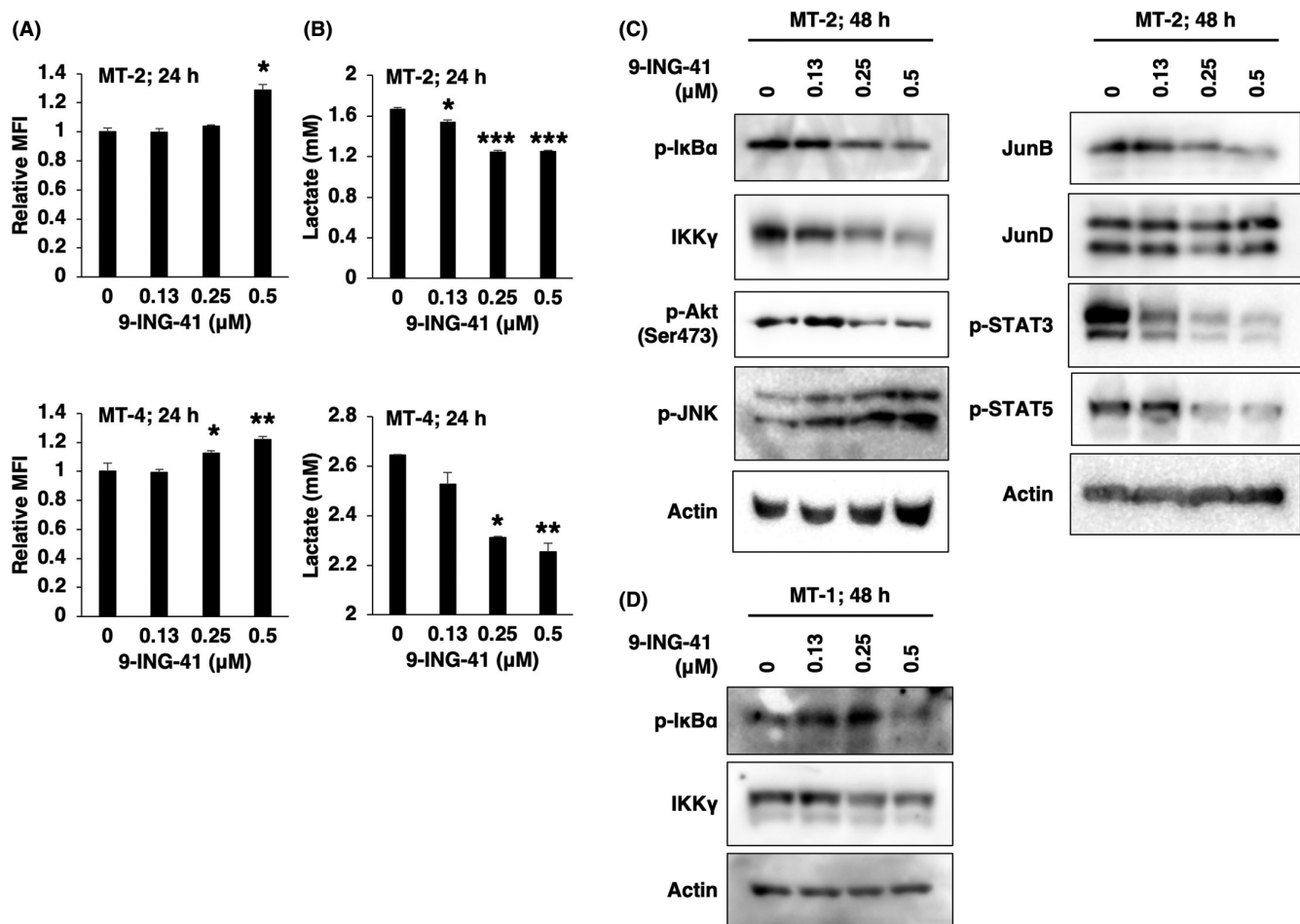


**FIGURE 6** | GSK-3 $\beta$  regulates reactive oxygen species (ROS) generation, glycolysis, and cell survival pathways. (A) The effect of 9-ING-41 on ROS generation. MT-2 and MT-4 cells were treated with the indicated concentrations of 9-ING-41 for 24 h. After treatment, the cells were incubated with CellROX fluorescent dye, and intracellular ROS levels were detected using flow cytometry. MFI: mean fluorescence intensity. Data represent the mean  $\pm$  SD of triplicate samples. \* $p$  < 0.05 and \*\* $p$  < 0.001, compared with the control. (B) 9-ING-41 treatment reduced lactate production. MT-2 and MT-4 cells were treated with the indicated concentrations of 9-ING-41 for 24 h and lactate production was analyzed. Data represent the mean  $\pm$  SD of triplicate samples. \* $p$  < 0.005, \*\* $p$  < 0.001, and \*\*\* $p$  < 0.00005, compared with the control. (C and D) Levels of proteins in the NF- $\kappa$ B, Akt, AP-1, STAT3/5, and JNK signaling pathways in MT-2 cells (C) and MT-1 cells (D) treated with 9-ING-41 for 48 h were determined using western blotting. Actin was used as a loading control.

overcome drug resistance in p53-null drug-resistant cancer cells by enabling necroptosis in response to chemotherapy [45]. Glycolysis is an important pathway for cellular energy production. The normal regulation of intracellular glucose metabolism plays an important role in tumor ferroptosis [46]. Previously, GSK-3 $\beta$  was demonstrated to be involved in the regulation of glycolysis in cancer cells [21]. Consistent with this report, levels of lactate, the end-product of glycolysis, were reduced in HTLV-1-infected T cells treated with 9-ING-41, suggesting that inhibition of glycolysis may be involved in the induction of ferroptosis by 9-ING-41. ATL has a dismal prognosis, with a median survival of less than 1 year, mainly due to its resistance to chemotherapy [2–4]. However, 9-ING-41, which promotes cell death by necroptosis and ferroptosis, may circumvent many of the prosurvival advantages of apoptosis-resistant ATL cells.

In our study, the IC<sub>50</sub> of 9-ING-41 at 72 h of administration was 77–636 nM. Pharmacokinetic studies showed that 9-ING-41 exhibits plasma concentrations above its in vitro IC<sub>50</sub> for more than 6 h after a single administration of 9.3 mg/kg [47]. These

results suggest that 9-ING-41 can directly inhibit the proliferation and survival of ATL cells in patients. In addition to their role in cancer cell proliferation and survival, GSK-3 inhibitors, including 9-ING-41, enhance CD8 cytotoxic T cell function by downregulating PD-1, TIGIT, and LSG-3 expression [48], and natural killer cell function by upregulating LFA expression [49] in mouse models. Furthermore, treatment of CD8 T cells derived from an ATL patient with 9-ING-41 increased the secretion of IFN- $\gamma$ , granzyme B, and TRAIL [12]. Thus, treatment with 9-ING-41 may enhance anti-ATL immune responses in ATL patients.

Targeting GSK-3 $\beta$  decreased the survival and proliferation of HTLV-1-infected T cells due to ROS production, DNA damage, activation of JNK and p53, inhibition of glycolysis, and suppression of c-Myc, NF- $\kappa$ B, AP-1, Akt, and STAT3/5 signaling (Figure S1). Although we did not use primary leukemic cells from ATL patients, these mechanistic insights into the roles of GSK-3 $\beta$  in HTLV-1-infected T-cell biology provide rationale for clinical studies in ATL patients.

---

## Author Contributions

Naoki Mori contributed to the conception and design of the study. Both authors contributed to the acquisition, analysis, and interpretation of the data in this study. The manuscript was written by Naoki Mori. Both authors approved the final version of the article and agreed to be accountable for all aspects of the work, ensuring that questions related to the accuracy or integrity of any part of this research are appropriately investigated and resolved.

## Acknowledgments

We would like to thank the Fujisaki Cell Center, Hayashibara Biochemical Laboratories, Inc. for providing HUT-102, MT-1, and Jurkat cells, Dr Naoki Yamamoto (Tokyo Medical and Dental University) for providing MT-2 and MT-4 cells, Dr Diane Prager (UCLA School of Medicine) for providing SLB-1 cells, Dr Masahiro Fujii (Niigata University) for providing TL-OmI cells, and Dr Yuetsu Tanaka (University of the Ryukyus) for providing the Lt-4 antibody. We also thank the University of the Ryukyus Center for Research Advancement and Collaboration for providing the facilities for flow cytometric analyses and assessment of protein concentrations, and Editage ([www.editage.jp](http://www.editage.jp)) for their assistance with English language editing.

## Ethics Statement

The authors have nothing to report.

## Conflicts of Interest

The authors declare no conflicts of interest.

## Data Availability Statement

The data generated in this study are available upon request from the corresponding author.

## References

1. J. I. Yasunaga, "Viral, Genetic, and Immune Factors in the Oncogenesis of Adult T-Cell Leukemia/Lymphoma," *International Journal of Hematology* 117 (2023): 504–511.
2. K. Tsukasaki, A. Marçais, R. Nasr, et al., "Diagnostic Approaches and Established Treatments for Adult T Cell Leukemia Lymphoma," *Frontiers in Microbiology* 11 (2020): 1207.
3. R. Hleihel, A. Akkouche, H. Skayneh, O. Hermine, A. Bazarbachi, and H. El Hajj, "Adult T-Cell Leukemia: A Comprehensive Overview on Current and Promising Treatment Modalities," *Current Oncology Reports* 23 (2021): 141.
4. H. Katsuya, "Current and Emerging Therapeutic Strategies in Adult T-Cell Leukemia-Lymphoma," *International Journal of Hematology* 117 (2023): 512–522.
5. A. Walz, A. Ugolkov, S. Chandra, et al., "Molecular Pathways: Revisiting Glycogen Synthase Kinase-3 $\beta$  as a Target for the Treatment of Cancer," *Clinical Cancer Research* 23 (2017): 1891–1897.
6. T. Domoto, M. Uehara, D. Bolidong, and T. Minamoto, "Glycogen Synthase Kinase 3 $\beta$  in Cancer Biology and Treatment," *Cells* 9 (2020): 1388.
7. C. Pecoraro, B. Faggion, B. Balboni, et al., "GSK3 $\beta$  as a Novel Promising Target to Overcome Chemoresistance in Pancreatic Cancer," *Drug Resistance Updates* 58 (2021): 100779.
8. C. Sutherland, "What Are the *Bona Fide* GSK3 Substrates?" *International Journal of Alzheimer's Disease* 2011 (2011): 505607.

9. R. Kurashina, J. H. Ohyashiki, C. Kobayashi, et al., "Anti-Proliferative Activity of Heat Shock Protein (Hsp) 90 Inhibitors via Beta-Catenin/TCF7L2 Pathway in Adult T Cell Leukemia Cells," *Cancer Letters* 284 (2009): 62–70.
10. H. Taniguchi, H. Hasegawa, D. Sasaki, et al., "Heat Shock Protein 90 Inhibitor NVP-AUY922 Exerts Potent Activity Against Adult T-Cell Leukemia-Lymphoma Cells," *Cancer Science* 105 (2014): 1601–1608.
11. C. Ishikawa, M. Senba, and N. Mori, "Efficiency of AUY922 in Mice With Adult T-Cell Leukemia/Lymphoma," *Oncology Letters* 12 (2016): 387–392.
12. A. Hsu, K. E. Huntington, A. De Souza, et al., "Clinical Activity of 9-ING-41, a Small Molecule Selective Glycogen Synthase Kinase-3 Beta (GSK-3 $\beta$ ) Inhibitor, in Refractory Adult T-Cell Leukemia/Lymphoma," *Cancer Biology & Therapy* 23 (2022): 417–423.
13. C. Zhang, Z. Ao, A. Seth, and S. F. Schlossman, "A Mitochondrial Membrane Protein Defined by a Novel Monoclonal Antibody Is Preferentially Detected in Apoptotic Cells," *Journal of Immunology* 157 (1996): 3980–3987.
14. C. Ishikawa, M. Senba, and N. Mori, "Importin  $\beta$ 1 Regulates Cell Growth and Survival During Adult T Cell Leukemia/Lymphoma Therapy," *Investigational New Drugs* 39 (2021): 317–329.
15. Y. Tanaka, A. Yoshida, Y. Takayama, et al., "Heterogeneity of Antigen Molecules Recognized by Anti-Tax<sub>1</sub> Monoclonal Antibody Lt-4 in Cell Lines Bearing Human T Cell Leukemia Virus Type I and Related Retroviruses," *Japanese Journal of Cancer Research* 81 (1990): 225–231.
16. Y. Tanaka, A. Yoshida, H. Tozawa, H. Shida, H. Nyunoya, and K. Shimotohno, "Production of a Recombinant Human T-Cell Leukemia Virus Type-I *Trans*-Activator (Tax<sub>1</sub>) Antigen and Its Utilization for Generation of Monoclonal Antibodies Against Various Epitopes on the Tax<sub>1</sub> Antigen," *International Journal of Cancer* 48 (1991): 623–630.
17. N. Mori, C. Ishikawa, and M. Senba, "Activation of PKC- $\delta$  in HTLV-1-Infected T Cells," *International Journal of Oncology* 46 (2015): 1609–1618.
18. J. M. Atkinson, K. B. Rank, Y. Zeng, et al., "Activating the Wnt/ $\beta$ -Catenin Pathway for the Treatment of Melanoma—Application of LY2090314, a Novel Selective Inhibitor of Glycogen Synthase Kinase-3," *PLoS One* 10 (2015): e0125028.
19. M. Piccolo, M. G. Ferraro, F. Iazzetti, R. Santamaria, and C. Irace, "Insight Into Iron, Oxidative Stress and Ferroptosis: Therapy Targets for Approaching Anticancer Strategies," *Cancers (Basel)* 16 (2024): 1220.
20. S. Galadari, A. Rahman, S. Pallichankandy, and F. Thayyullathil, "Reactive Oxygen Species and Cancer Paradox: To Promote or to Suppress?" *Free Radical Biology & Medicine* 104 (2017): 144–164.
21. G. Fang, P. Zhang, J. Liu, et al., "Inhibition of GSK-3 $\beta$  Activity Suppresses HCC Malignant Phenotype by Inhibiting Glycolysis via Activating AMPK/mTOR Signaling," *Cancer Letters* 463 (2019): 11–26.
22. R. Sasaki, S. Ito, M. Asahi, and Y. Ishida, "YM155 Suppresses Cell Proliferation and Induces Cell Death in Human Adult T-Cell Leukemia/Lymphoma Cells," *Leukemia Research* 39 (2015): 1473–1479.
23. A. M. Martelli, F. Paganelli, C. Evangelisti, F. Chiarini, and J. A. McCubrey, "Pathobiology and Therapeutic Relevance of GSK-3 in Chronic Hematological Malignancies," *Cells* 11 (2022): 1812.
24. J. Wei, J. Wang, J. Zhang, J. Yang, G. Wang, and Y. Wang, "Development of Inhibitors Targeting Glycogen Synthase Kinase-3 $\beta$  for Human Diseases: Strategies to Improve Selectivity," *European Journal of Medicinal Chemistry* 236 (2022): 114301.
25. O. H. M. Elmadbouh, S. J. Pandol, and M. Edderkaoui, "Glycogen Synthase Kinase 3 $\beta$ : A True Foe in Pancreatic Cancer," *International Journal of Molecular Sciences* 23 (2022): 14133.

26. A. F. Serpico and D. Grieco, "Recent Advances in Understanding the Role of Cdk1 in the Spindle Assembly Checkpoint," *F1000Res* 9 (2020): F1000.
27. B. D. Xiao, Y. J. Zhao, X. Y. Jia, J. Wu, Y. G. Wang, and F. Huang, "Multifaceted p21 in Carcinogenesis, Stemness of Tumor and Tumor Therapy," *World Journal of Stem Cells* 12 (2020): 481–487.
28. G. Bretones, M. D. Delgado, and J. León, "Myc and Cell Cycle Control," *Biochimica et Biophysica Acta* 1849 (2015): 506–516.
29. A. S. Gomes, H. Ramos, J. Soares, and L. Saraiva, "p53 and Glucose Metabolism: An Orchestra to Be Directed in Cancer Therapy," *Pharmacological Research* 131 (2018): 75–86.
30. R. Karmali, V. Chukkapalli, L. I. Gordon, et al., "GSK-3 $\beta$  Inhibitor, 9-ING-41, Reduces Cell Viability and Halts Proliferation of B-Cell Lymphoma Cell Lines as a Single Agent and in Combination With Novel Agents," *Oncotarget* 8 (2017): 114924–114934.
31. S. Goldar, M. S. Khaniani, S. M. Derakhshan, and B. Baradaran, "Molecular Mechanisms of Apoptosis and Roles in Cancer Development and Treatment," *Asian Pacific Journal of Cancer Prevention* 16 (2015): 2129–2144.
32. J. M. Taylor and C. Nicot, "HTLV-1 and Apoptosis: Role in Cellular Transformation and Recent Advances in Therapeutic Approaches," *Apoptosis* 13 (2008): 733–747.
33. H. Gazon, B. Barbeau, J. M. Mesnard, and J. M. Peloponese, Jr., "Hijacking of the AP-1 Signaling Pathway During Development of ATL," *Frontiers in Microbiology* 8 (2018): 2686.
34. T. A. Waldmann, "JAK/STAT Pathway Directed Therapy of T-Cell Leukemia/Lymphoma: Inspired by Functional and Structural Genomics," *Molecular and Cellular Endocrinology* 451 (2017): 66–70.
35. D. Verzella, A. Pescatore, D. Capece, et al., "Life, Death, and Autophagy in Cancer: NF- $\kappa$ B Turns Up Everywhere," *Cell Death & Disease* 11 (2020): 210.
36. C. Recio, B. Guerra, M. Guerra-Rodríguez, et al., "Signal Transducer and Activator of Transcription (STAT)-5: An Opportunity for Drug Development in Oncohematology," *Oncogene* 38 (2019): 4657–4668.
37. M. Pakjoo, S. E. Ahmadi, M. Zahedi, et al., "Interplay Between Proteasome Inhibitors and NF- $\kappa$ B Pathway in Leukemia and Lymphoma: A Comprehensive Review on Challenges Ahead of Proteasome Inhibitors," *Cell Communication and Signaling: CCS* 22 (2024): 105.
38. S. Medunjanin, L. Schleithoff, C. Fiegehenn, S. Weinert, W. Zschratter, and R. C. Braun-Dullaeus, "GSK-3 $\beta$  Controls NF-kappaB Activity via IKK $\gamma$ /NEMO," *Scientific Reports* 6 (2016): 38553.
39. C. Gao, X. Yuan, Z. Jiang, et al., "Regulation of AKT Phosphorylation by GSK3 $\beta$  and PTEN to Control Chemoresistance in Breast Cancer," *Breast Cancer Research and Treatment* 176 (2019): 291–301.
40. E. Beurel and R. S. Jope, "Differential Regulation of STAT Family Members by Glycogen Synthase Kinase-3," *Journal of Biological Chemistry* 283 (2008): 21934–21944.
41. S. Gao, S. Li, X. Duan, et al., "Inhibition of Glycogen Synthase Kinase 3 Beta (GSK3 $\beta$ ) Suppresses the Progression of Esophageal Squamous Cell Carcinoma by Modifying STAT3 Activity," *Molecular Carcinogenesis* 56 (2017): 2301–2316.
42. L. Wang, Y. Wang, Y. Meng, C. Zhang, and L. Di, "GSK3-Activated STAT5 Regulates Expression of SFRPs to Modulate Adipogenesis," *FASEB Journal* 32 (2018): 4714–4726.
43. T. Gomard, H. A. Michaud, D. Tempé, K. Thiolon, M. Pelegrin, and M. Piechaczyk, "An NF-kappaB-Dependent Role for JunB in the Induction of Proinflammatory Cytokines in LPS-Activated Bone Marrow-Derived Dendritic Cells," *PLoS One* 5 (2010): e9585.
44. M. R. Sepand, S. Ranjbar, I. M. Kempson, et al., "Targeting Non-Apoptotic Cell Death in Cancer Treatment by Nanomaterials: Recent Advances and Future Outlook," *Nanomedicine* 29 (2020): 102243.
45. E. Grassilli, R. Narloch, E. Federzoni, et al., "Inhibition of GSK3B Bypass Drug Resistance of p53-Null Colon Carcinomas by Enabling Necroptosis in Response to Chemotherapy," *Clinical Cancer Research* 19 (2013): 3820–3831.
46. X. Jiang, Q. Peng, M. Peng, et al., "Cellular Metabolism: A Key Player in Cancer Ferroptosis," *Cancer Communications* 44 (2024): 185–204.
47. B. A. Carneiro, L. Cavalcante, D. Mahalingam, et al., "Phase I Study of Elraglusib (9-ING-41), a Glycogen Synthase Kinase-3 $\beta$  Inhibitor, As Monotherapy or Combined With Chemotherapy in Patients With Advanced Malignancies," *Clinical Cancer Research* 30 (2024): 522–531.
48. G. Shaw, L. Cavalcante, F. J. Giles, and A. Taylor, "Elraglusib (9-ING-41), a Selective Small-Molecule Inhibitor of Glycogen Synthase Kinase-3 Beta, Reduces Expression of Immune Checkpoint Molecules PD-1, TIGIT and LAG-3 and Enhances CD8<sup>+</sup> T Cell Cytolytic Killing of Melanoma Cells," *Journal of Hematology & Oncology* 15 (2022): 134.
49. R. Parameswaran, P. Ramakrishnan, S. A. Moreton, et al., "Repression of GSK3 Restores NK Cell Cytotoxicity in AML Patients," *Nature Communications* 7 (2016): 11154.

### Supporting Information

Additional supporting information can be found online in the Supporting Information section.